

## ORIGINAL ARTICLE

# Correlation between dynamic CT findings and pathological prognostic factors of small lung adenocarcinoma

Shingo Iwano, Wataru Koike, Keiji Matsuo, Mariko Kitano, Kenichi Kawakami, Tohru Okada, Shinji Naganawa

Department of Radiology, Nagoya University Graduate School of Medicine, 65 Tsurumai-cho, Showa-ku, Nagoya 4668550, Japan

Corresponding address: Shingo Iwano, Department of Radiology, Nagoya University Graduate School of Medicine, 65 Tsurumai-cho, Showa-ku, Nagoya 4668550, Japan.

Email: iwano45@med.nagoya-u.ac.jp

Date accepted for publication 20 February 2012

### Abstract

**Abstract Purpose:** To compare pathological prognostic factors of small lung adenocarcinomas with findings of contrast-enhanced dynamic computed tomography (CT) scans. **Materials and methods:** We evaluated 108 patients with lung adenocarcinomas  $\leq 30$  mm in diameter who underwent dynamic CT scans (80–96 ml of contrast material, 2.5–3 ml/s injection) and tumor resections. Attenuation values of both the early phase (20–36 s after injection) and delayed phase (91–95 s) of enhanced CT minus baseline plain CT attenuation were defined as  $\Delta$ Early and  $\Delta$ Delay. The early enhancement ratio was defined as  $\Delta$ Early/ $\Delta$ Delay  $\times 100$  (%). We statistically compared the early enhancement ratios between the presence and absence of each pathological finding (lymph node metastasis, lymphatic permeation, vascular invasion, and pleural involvement). Patients were divided into 2 groups based on early enhancement ratios: ratio  $\geq 50\%$  ( $n = 41$ ) and ratio  $< 50\%$  ( $n = 67$ ) and we statistically compared these 2 groups. **Results:** The early enhancement ratios in the group with lymph node metastasis, lymphatic permeation, and vascular invasion were significantly lower than in the group without these findings (24.9% vs 48.6%;  $P < 0.001$ , 30.0% vs 47.5%;  $P = 0.002$ , and 26.5% vs 47.0%;  $P = 0.002$ , respectively). Lymph node metastasis, lymphatic permeation, and vascular invasion were significantly more frequent in tumors with a ratio  $< 50\%$  than in tumors with ratio  $\geq 50\%$  ( $P < 0.001$ ,  $P = 0.008$ , and  $P = 0.005$ , respectively). **Conclusions:** There was a significant correlation between the early enhancement ratio of enhanced dynamic CT and the pathological prognostic factors in small lung adenocarcinomas.

**Keywords:** Adenocarcinoma; dynamic CT; lung neoplasms; multidetector row CT; prognostic factor.

## Introduction

Contrast-enhanced dynamic computed tomography (CT) scans of lung cancers provide non-invasive quantitative information regarding perfusion patterns that can be used for the differential diagnosis between malignant and benign pulmonary lesions<sup>[1–7]</sup>. Moreover, Shim et al.<sup>[8]</sup> showed that peak enhancement of 110 Hounsfield units (HU) of stage T1 lung cancers on dynamic CT were significantly associated with the presence of mediastinal or hilar nodal metastasis.

However, dynamic CT findings of lung adenocarcinoma are affected not only by tumor angiogenesis but also by fibrosis within the tumor. In a recent study, Iwano et al.<sup>[9]</sup> showed that the degree of fibrosis within a stage I lung adenocarcinoma tumor could affect the enhanced pattern on dynamic CT. That is, there was a negative correlation between the amount of fibrosis and the enhancement grade at the early phase of contrast-enhanced dynamic CT in solid types of lung adenocarcinomas. In addition, Maeshima et al.<sup>[10]</sup> reported that the degree of fibrosis within a tumor was a useful prognostic

factor for patients with small lung adenocarcinomas (maximum diameter  $\leq 30$  mm). This indicated that preoperative dynamic CT may be able to noninvasively predict the prognoses of patients with small lung adenocarcinomas.

Therefore, in this study, we focused on the pathological prognostic factors (lymph node metastasis, lymphatic permeation, vascular invasion, and pleural involvement) of small lung adenocarcinomas and compared these results with the findings of contrast-enhanced dynamic CT scans.

## Materials and methods

This retrospective study was approved by our institutional review board with a waiver for informed consent.

### Patients

We reviewed the medical records, postoperative pathological records, and preoperative multidetector row computed tomography (MDCT) images of patients who underwent surgical lung resections for primary lung adenocarcinomas  $\leq 30$  mm in diameter in our hospital between May 2006 and December 2010. Hilar lung adenocarcinomas and nonsolid types of adenocarcinoma that were invisible on mediastinal window settings for thoracic CT were excluded. Patients heavier than 80 kg were also excluded because the concentration of contrast medium used per unit body mass was lower. We recorded patient characteristics (age and body weight) from medical records and tumor characteristics (size, location, scar grade, and TNM classification (Union for International Cancer Control (UICC) 7th edition) from pathological records. The scar grade based on the report of Maeshima et al.<sup>[10]</sup> is recorded routinely in our hospital in the pathological records as an index of fibrosis in adenocarcinoma: grade 1, adenocarcinoma without a desmoplastic reaction; grade 2, sparse desmoplastic reaction; grade 3, dense desmoplastic reaction with diameter of  $\leq 10$  mm; grade 4, dense desmoplastic reaction with diameter  $> 10$  mm.

We selected 108 consecutive patients with small peripheral lung adenocarcinomas for analysis (68 males and 40 females; mean age 67 years; age range 43–84 years). Patient and tumor characteristics are summarized in Table 1. The mean period between a dynamic CT and thoracic surgery was 23 days.

### Contrast-enhanced dynamic CT scan protocol

All CT scans were performed with a 64-channel MDCT scanner (Aquilion64; Toshiba Medical Systems, Tokyo, Japan) in the craniocaudal direction with inspiratory apnea. The scanning parameters were 120 kV and auto mA (max. 450 mA). The gantry rotation time was 0.5 s. The reconstruction thickness was 1 mm using a standard

**Table 1 Characteristics of patients and tumors**

Characteristics	Value
Age (years), mean $\pm$ SD	67 $\pm$ 8
Body weight (kg), mean $\pm$ SD	56.8 $\pm$ 9.2
Tumor size (mm), mean $\pm$ SD	20.6 $\pm$ 5.9
Pulmonary lobe ( <i>n</i> )	
Right upper lobe	41
Right middle lobe	6
Right lower lobe	19
Left upper lobe	26
Left lower lobe	16
Pathological stage ( <i>n</i> )	
I	84
II	12
III	11
IV	1
Scar grade ( <i>n</i> )	
Grade 1	26
Grade 2	55
Grade 3	18
Grade 4	9

algorithm. The volume CT dose index (CTDI<sub>vol</sub>) was about 30 mGy for one scan. Iodine calibration was not performed; routine calibration against air and water was performed in accordance with the manufacturers' recommendations<sup>[11]</sup>.

Vascular access was by a cubital vein with a 20-G needle. For vessel enhancement, 96 ml of nonionic contrast medium (Optiray 320, 320 mg I/ml ioversol, Tyco Healthcare, Tokyo, Japan, or Iopamiron 370, 370 mg I/ml iopamidol, Bayer Healthcare, Tokyo, Japan) was used at a flow rate of 3.0 ml/s. Ioversol was used for 71 patients with body weight  $\leq 60$  kg and iopamidol was used for 34 patients with body weight  $> 60$  kg. For 3 patients with body weights  $\leq 40$  kg, 80 ml of ioversol was used at a flow rate of 2.5 ml/s. The injection was immediately followed by a saline chaser bolus of 24 ml at the same flow rate using a dual-barrel power injector (Dual Shot GX, Nemoto Kyorindo, Tokyo, Japan).

For the early phase, the scan delay was evaluated by an automatic bolus tracking system with a circular region of interest (ROI) localized on the descending aorta at the level of tracheal bifurcation. Scanning started automatically when the attenuation of the ROI reached 150 HU. For the delayed phase, the scan delay was 90 s after the start of contrast medium injection. This preoperative CT scan protocol was approved as a routine scan by an institutional conference comprised of respiratory medicine, thoracic surgery and radiology.

### Analysis of dynamic contrast-enhanced CT images

CT images were displayed on a commercial PACS viewer (Rapideye Station, Toshiba Medical Systems, Tokyo, Japan) at mediastinal window settings (window width

of 350 HU and window center of 40 HU). For the quantitative analysis of each CT image, the ROIs were placed on 3 images of 1-mm slice thickness in the central part of the tumor, and the median value of 3 ROIs was recorded. A chest radiologist with 16 years of experience reading thoracic CTs drew polygonal ROIs over the tumor without knowledge of the pathological findings. The ROI was drawn as large as possible in order to minimize noise, but care was taken to avoid partial volume effects (Figs. 1–3). To avoid interfusion of air space, the reader magnified the image for display on the viewer, and drew the lines of ROIs inside the boundary of tumors. The ROIs were confirmed by another radiologist. The attenuation values of both the early phase and the delayed phase of enhanced CT minus the baseline plain CT attenuation were defined as  $\Delta$ Early and  $\Delta$ Delay. The early enhancement ratio was defined as  $\Delta$ Early/ $\Delta$ Delay $\times$ 100 (%). The early enhancement ratio indicated the proportion of early to delayed enhancement. Thus, tumors with a high early enhancement ratio were substantially enhanced in the early phase. At the same time, the delay times of the enhanced CT images on which ROIs were drawn were recorded from the DICOM image tag.

### Statistical analysis

We statistically compared the early enhancement ratios between the presence and absence of each pathological finding (lymph node metastasis, lymphatic permeation, vascular invasion, and pleural involvement) by *t* tests. Patients were then divided into 2 groups based on the early enhancement ratio: early enhancement (early enhancement ratio  $\geq$ 50%,  $n=41$ ) and delayed

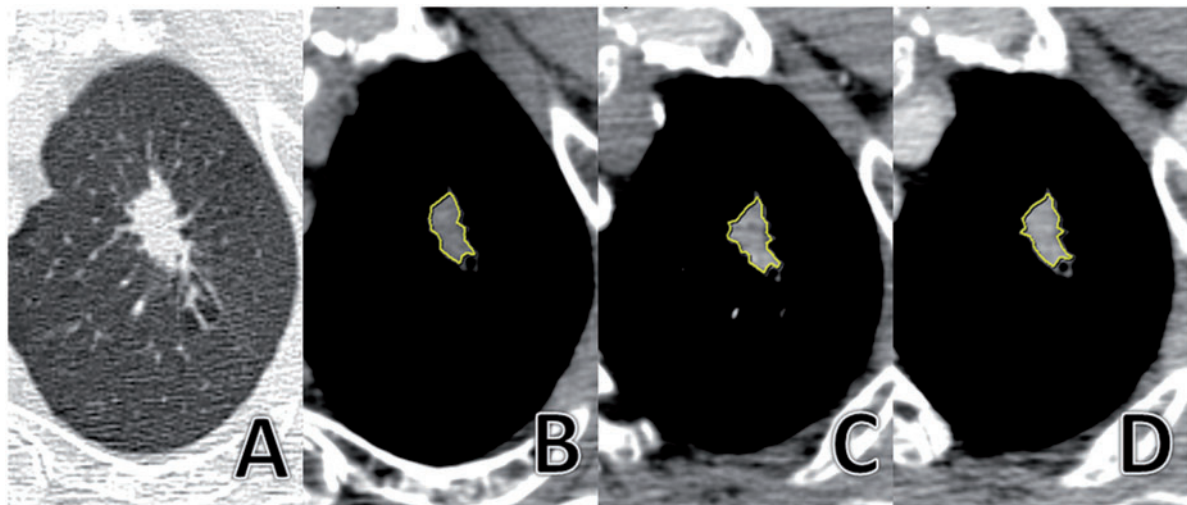
enhancement (early enhancement ratio  $<$ 50%,  $n=67$ ). We statistically compared these 2 groups. Clinical characteristics (age, weight, and tumor size) were compared by *t* tests. Pathological findings were compared by chi-square tests. Scar grades were compared by Mann–Whitney *U* tests. Excel 2007 (Microsoft Corp., Redmond, WA) and SPSS version 16 (SPSS, Inc., Chicago, IL) were used for analyses. A *P* value  $<$ 0.05 was considered statistically significant.

### Results

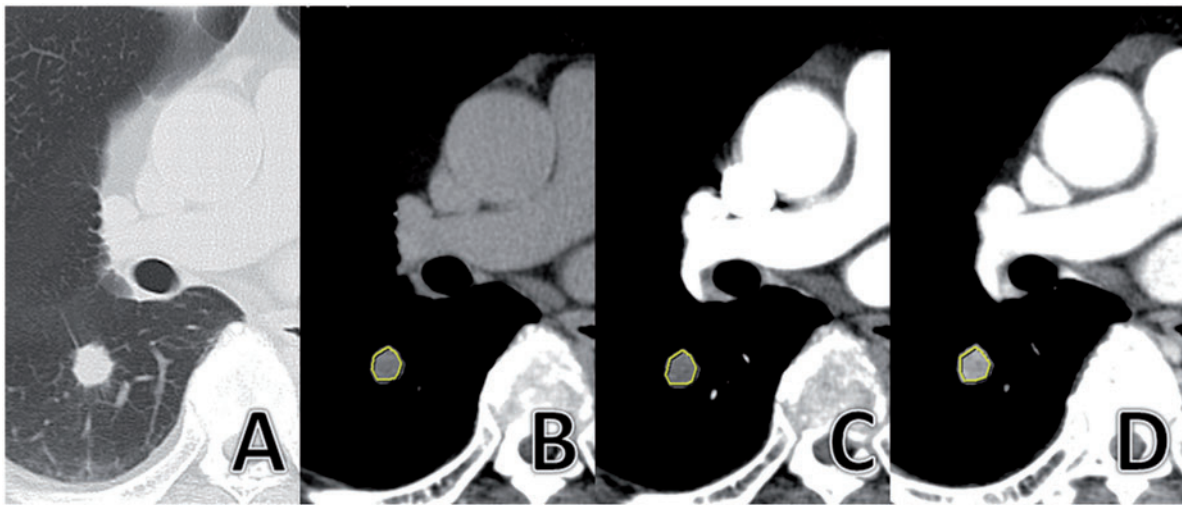
For all adenocarcinomas evaluated, the mean  $\pm$  SD of  $\Delta$ Early,  $\Delta$ Delay, and the early enhancement ratio were  $20 \pm 15$  HU,  $45 \pm 18$  HU, and  $44 \pm 32\%$ , respectively. The scan delay times ranged from 20 to 36 s (mean = 27 s) at the early phase and from 91 to 95 s (mean = 92 s) at the delayed phase.

Table 2 shows the results for the early enhancement ratios for the presence and absence of 4 pathological findings. The early enhancement ratio in the group with lymph node metastasis was significantly lower than that in the group without lymph node metastasis ( $P < 0.001$ ). The early enhancement ratio in the group with lymphatic permeation was significantly lower than that in the group without lymphatic permeation ( $P = 0.002$ ). The early enhancement ratio in the group with vascular invasion was significantly lower than that in the group without vascular invasion ( $P = 0.002$ ). The early enhancement ratio in the group with pleural involvement was lower than that in the group without pleural involvement, although the difference was not significant ( $P = 0.089$ ).

Table 3 shows the results for comparisons between early enhancement tumors and delayed enhancement



**Figure 1** (A) Adenocarcinoma tumor of scar grade 2 in the left upper lobe. (B) The CT attenuation value before contrast injection was 27 HU. (C) The attenuation value at early phase was 61 HU. (D) The attenuation value at delayed phase was 68 HU. The early enhancement ratio was 82.9%. Lymph node metastasis, lymphatic permeation, vascular invasion, and pleural involvement were not observed in the pathological findings. The yellow lines show the ROI settings.



**Figure 2** (A) Adenocarcinoma tumor of scar grade 3 in the right lower lobe. (B) The CT attenuation value before contrast injection was 24 HU. (C) The attenuation value at early phase was 46 HU. (D) The attenuation value at delayed phase was 72 HU. The early enhancement ratio was 45.8%. Lymphatic permeation, and vascular invasion, and pleural involvement were observed in the pathological findings. The yellow lines show the ROI settings.

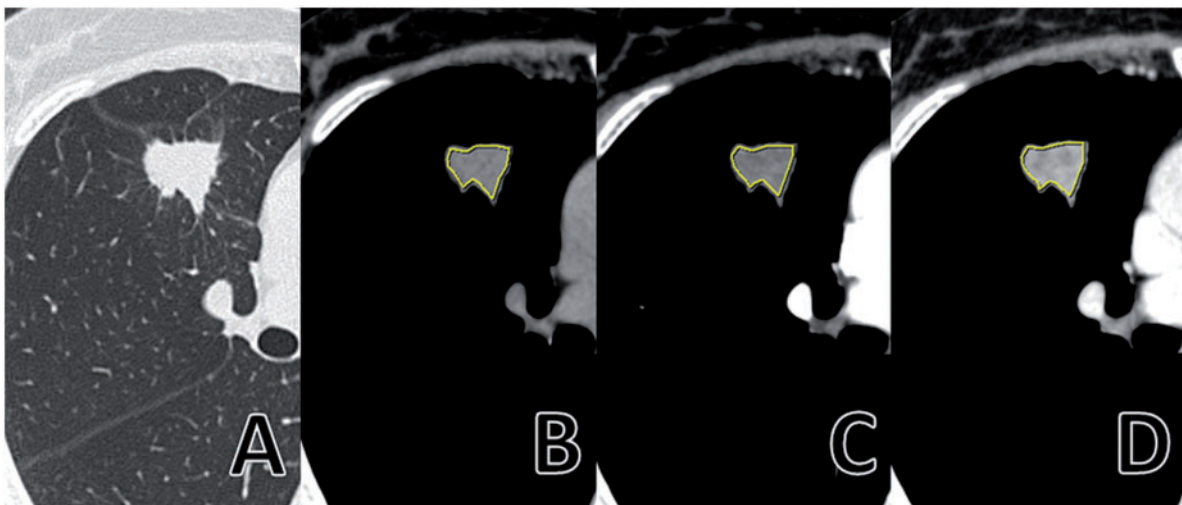


**Figure 3** (A) Adenocarcinoma tumor of scar grade 3 in the right upper lobe. (B) The CT attenuation value before contrast injection was 34 HU. (C) The attenuation value at early phase was 47 HU. (D) The attenuation value at delayed phase was 71 HU. The early enhancement ratio was 35.1%. Mediastinal lymph node metastasis, lymphatic permeation, vascular invasion, and pleural involvement were observed in the pathological findings. The yellow lines show the ROI settings.

tumors. There were no significant differences between the 2 groups for patients' characteristics (age, body weight) and tumor size. For the pathological findings, lymph node metastasis, lymphatic permeation, and vascular invasion were significantly more frequent in the delayed enhancement tumors than in the early enhancement tumors ( $P < 0.001$ ,  $P = 0.008$ , and  $P = 0.005$ , respectively). However, there were no significant differences between the 2 groups for pleural involvement ( $P = 0.515$ ). In addition, higher scar grade neoplasms

were significantly more frequent in the delayed enhancement neoplasms ( $P = 0.001$ ; Fig. 4).

## Discussion

Lung adenocarcinomas typically have varying amounts of fibrosis. Several histopathological studies have shown that the amounts of intratumoral fibrosis were significantly correlated with patients' prognoses. Noguchi

**Table 2 Comparisons of early enhancement ratios between the presence and absence of pathological findings**

Pathological findings	Present(+) or absent (-)	<i>n</i>	Early enhancement ratio (%)	<i>P</i> value
Lymph node metastasis	(+)	21	24.9 ± 16.1	<0.001
	(-)	87	48.6 ± 33.5	
Lymphatic permeation	(+)	22	30.0 ± 18.2	0.002
	(-)	86	47.5 ± 34.1	
Vascular invasion	(+)	16	26.5 ± 20.1	0.002
	(-)	92	47.0 ± 33.1	
Pleural involvement	(+)	57	39.0 ± 29.4	0.089
	(-)	51	49.5 ± 34.6	

*P* values were determined by *t* tests.

**Table 3 Comparisons between early enhancement tumors (early enhancement ratio ≥50%) and delayed enhancement tumors (early enhancement ratio <50%)**

	Early enhancement tumors	Delayed enhancement tumors	<i>P</i> value
Number of cases	41	67	
Age (years)	67 ± 9	67 ± 7	0.687
Weight (kg)	58.9 ± 10.0	55.5 ± 8.6	0.067
Tumor size (mm)	19.3 ± 6.1	21.4 ± 5.7	0.079
Pathological findings			
Lymph node metastasis (N1–2)	1 (2.4)	20 (29.9)	<0.001
Lymphatic permeation (ly1)	3 (7.3)	19 (28.4)	0.008
Vascular invasion (v1)	1 (2.4)	15 (22.4)	0.005
Pleural involvement (p1–3)	20 (48.8)	37 (55.2)	0.515

Numbers in parentheses are percentages. *P* values for age, weight, and tumor size were determined by *t* tests. *P* values for pathological findings were determined by chi-square tests.

et al.<sup>[12]</sup> classified small lung adenocarcinomas into 6 subtypes based on tumor growth patterns and showed that active fibroblastic proliferation in the scar was an important prognostic factor for peripheral-type small adenocarcinomas of the lung. Maeshima et al.<sup>[10]</sup> adopted the scar grade as a semi-quantitative index of fibrosis within lung adenocarcinoma and reported that it was significantly correlated with the pathological stage and prognosis of patients with small adenocarcinomas in the lung. In addition, they reported that the relationship between the scar grades was significantly associated with lymph node metastasis, lymphatic permeation, vascular invasion, and pleural invasion. Therefore, if we can non-invasively evaluate the degree of intratumoral fibrosis and the prognosis based on preoperative diagnostic imaging, it may be useful for planning the therapeutic strategies for patients with small adenocarcinomas. Many investigators have reported that nonsolid type adenocarcinomas on high-resolution CT, which included no fibrosis, had better prognoses<sup>[13–15]</sup>. However, there has been little in the way of radiological methods to quantify the amounts of intratumoral fibrosis in solid types of lung adenocarcinomas.

The early enhancement ratio is valuable for evaluating intratumoral fibrosis<sup>[9]</sup>. Contrast enhancement of small

lung adenocarcinomas in the early phase, when the contrast agent is predominantly in the intravascular component, is negatively correlated with the degrees of fibrosis within the neoplasms. This may result from the smaller intratumoral blood spaces and blood flow in those neoplasms with abundant fibrosis, resulting in an absolutely lower volume of contrast inflow into this type of tumor. In contrast, when there are enhancements in the delayed phase, when contrast enhancement depends primarily on extravascular–extracellular components, neoplasms with abundant internal fibrosis show prominent enhancement in the delayed phase due to an increased extravascular–extracellular component<sup>[1]</sup>. Therefore, the early enhancement ratio can reflect the amount of intratumoral fibrosis.

Iwano et al.<sup>[9]</sup> showed that contrast-enhanced dynamic CT findings could semi-quantify fibrosis in solid and partly solid types of adenocarcinomas. That is, the early enhancement ratio of a dynamic CT was significantly and negatively correlated with the degree of fibrosis within the neoplasms. Therefore, we also adopted the early enhancement ratio as an index of intratumoral contrast enhancement in the present study. As a result, the group of delayed enhancement neoplasms with early enhancement ratios <50% included significantly more

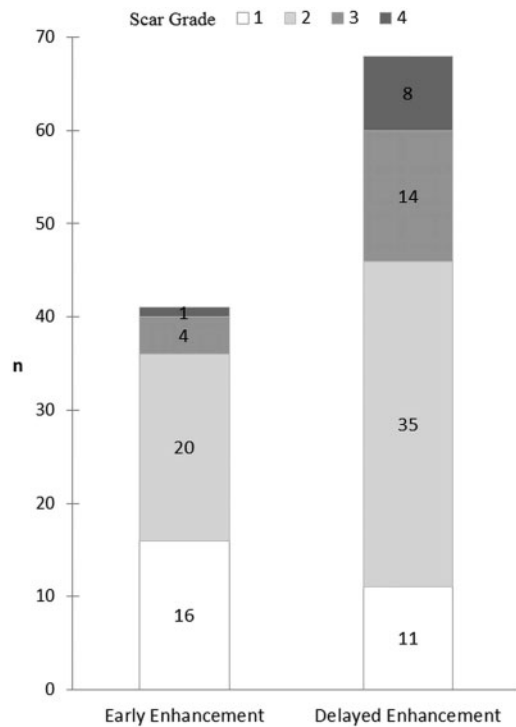


**Figure 4** Bar chart showing the numbers of each scar grade of adenocarcinomas in the early enhancement group ( $n=41$ ) and delayed enhancement group ( $n=67$ ). Higher scar grade neoplasms were significantly more frequent in the delayed enhancement neoplasms ( $P=0.001$ ).

adenocarcinomas with extensive fibrosis. As noted above, Maeshima et al.<sup>[10]</sup> reported that the degree of fibrosis within small lung adenocarcinomas was significantly correlated with the pathological stage and the prognosis of the patients. They indicated that a preoperative dynamic CT could noninvasively predict the prognosis of patients with lung adenocarcinoma. Therefore, in the present study, we also investigated the possible correlation between the preoperative dynamic CT findings and the postoperative histopathological findings that affect prognosis.

Based on our results, our prediction has turned out to be correct. The early enhancement ratios of neoplasms that had lymph node metastasis, lymphatic permeation, and vascular invasion were significantly lower. In addition, in those neoplasms with low early enhancement ratios (<50%), lymph node metastasis, lymphatic permeation, and vascular invasion were significantly more frequent. These findings indicate that dynamic CT findings of small adenocarcinoma are useful for predicting prognosis. In addition, a dynamic CT may be able to noninvasively evaluate intratumoral fibrosis and predict prognosis before surgery; the scar grade can predict prognosis only after surgery. Our data demonstrated that even a small adenocarcinoma could metastasize to hilar or

mediastinal lymph nodes. If we can predict high invasiveness of a tumor by preoperative dynamic CT findings, we may prevent residual lymph node metastases by means of proper removal of the lymph nodes.

The early enhancement ratio was significantly correlated with vascular and lymphatic vessel invasion, but was not significantly correlated with pleural involvement. We suggest the reason is that pleural involvement is influenced not only by tumor progression but also by the distance between the tumor and the pleura. In addition, the early enhancement ratio might reflect factors involved with tumor vessel invasion. Several studies have reported that vascular endothelial growth factor (VEGF), which promotes proliferation of tumor blood and lymphatic vessels, affected the dynamic CT findings of lung adenocarcinomas<sup>[16–18]</sup>. Further investigation is needed to determine the relationship between fibrosis and angiogenesis in lung adenocarcinoma.

This retrospective study has 3 limitations. First, we reviewed postoperative pathological records to evaluate the pathological prognostic factors, although we did not evaluate survival rates after surgery. However, many studies have provided evidence that lymph node metastasis, lymphatic permeation, and vascular invasion are prognostic factors for peripheral lung adenocarcinomas. Second, we investigated dual-phase dynamic scans using single-source MDCT in this study. Recently, several studies have demonstrated the usefulness of perfusion CT imaging using dual-source MDCT for the differentiation between benign and malignant lesions and the assessment of tumor angiogenesis<sup>[19–23]</sup>. Perfusion CT imaging may allow more accurate evaluation of angiogenesis in lung adenocarcinoma. Third, we could not use automatic segmentation software to measure the attenuation value of whole tumor. As an alternative, we measured the 3 ROIs in the central part of the tumor. Therefore, our results may contain some measurement error although the ROI was drawn as large as possible in order to minimize noise, but care was taken to avoid partial volume effects.

In conclusion, there was a significant correlation between the early enhancement ratio of enhanced dynamic CT and the pathological prognostic factors of small lung adenocarcinomas. In those tumors with low early enhancement ratios (<50%), lymph node metastasis, lymphatic permeation, and vascular invasion were significantly more frequent. Dynamic CT findings were modified by the degree of fibrosis within a lung tumor.

## Acknowledgement

We thank Dr Yoshie Shimoyama for providing histopathological reports.

## References

- [1] Hattori Y, Gabata T, Matsui O, et al. Enhancement patterns of pancreatic adenocarcinoma on conventional dynamic

- multi-detector row CT: correlation with angiogenesis and fibrosis. *World J Gastroenterol* 2009; 15: 3114–3121. doi:10.3748/wjg.15.3114.
- [2] Hata H, Mori H, Matsumoto S, et al. Fibrous stroma and vascularity of pancreatic carcinoma: correlation with enhancement patterns on CT. *Abdom Imaging* 2010; 35: 172–180. doi:10.1007/s00261-008-9460-0.
- [3] Lacomis JM, Baron RL, Oliver JH 3rd, Nalesnik MA, Federle MP. Cholangiocarcinoma: delayed CT contrast enhancement patterns. *Radiology* 1997; 203: 98–104.
- [4] Muramatsu Y, Takayasu K, Moriyama N, et al. Peripheral low-density area of hepatic tumors: CT-pathologic correlation. *Radiology* 1986; 160: 49–52.
- [5] Furukawa H, Takayasu K, Mukai K, et al. Late contrast-enhanced CT for small pancreatic carcinoma: delayed enhanced area on CT with histopathological correlation. *Hepatogastroenterology* 1996; 43: 1230–1237.
- [6] Yoshikawa J, Matsui O, Kadoya M, Gabata T, Arai K, Takashima T. Delayed enhancement of fibrotic areas in hepatic masses: CT-pathologic correlation. *J Comput Assist Tomogr* 1992; 16: 206–211. doi:10.1097/00004728-199203000-00006.
- [7] Bayraktaroglu S, Savas R, Basoglu OK, et al. Dynamic computed tomography in solitary pulmonary nodules. *J Comput Assist Tomogr* 2008; 32: 222–227. doi:10.1097/RCT.0b013e318136e29d.
- [8] Shim SS, Lee KS, Chung MJ, Kim H, Kwon OJ, Kim S. Do hemodynamic studies of stage T1 lung cancer enable the prediction of hilar or mediastinal nodal metastasis? *AJR Am J Roentgenol* 2006; 186: 981–988. doi:10.2214/AJR.04.1858.
- [9] Iwano S, Koike W, Matsuo K, Okada T, Shimoyama Y, Naganawa S. Correlation between dual-phase dynamic multi-detector CT findings and fibrosis within lung adenocarcinoma tumors. *Eur J Radiol* 2011; 80: e470–e475. doi:10.1016/j.ejrad.2010.09.007.
- [10] Maeshima AM, Niki T, Maeshima A, Yamada T, Kondo H, Matsuno Y. Modified scar grade: a prognostic indicator in small peripheral lung adenocarcinoma. *Cancer* 2002; 95: 2546–2554. doi:10.1002/cncr.11006.
- [11] Miles KA, Young H, Chica SL, Esser PD. Quantitative contrast-enhanced computed tomography: is there a need for system calibration? *Eur Radiol* 2007; 17: 919–926. doi:10.1007/s00330-006-0424-x.
- [12] Noguchi M, Morikawa A, Kawasaki M, et al. Small adenocarcinoma of the lung. Histologic characteristics and prognosis. *Cancer* 1995; 75: 2844–2852. doi:10.1002/1097-0142(19950615)75:12<2844::AID-CNCR2820751209>3.0.CO;2#.
- [13] Matsuguma H, Nakahara R, Anraku M, et al. Objective definition and measurement method of ground-glass opacity for planning limited resection in patients with clinical stage IA adenocarcinoma of the lung. *Eur J Cardiothorac Surg* 2004; 25: 1102–1106. doi:10.1016/j.ejcts.2004.02.004.
- [14] Hashizume T, Yamada K, Okamoto N, et al. Prognostic significance of thin-section CT scan findings in small-sized lung adenocarcinoma. *Chest* 2008; 133: 441–447. doi:10.1378/chest.07-1533.
- [15] Saito H, Kameda Y, Masui K, et al. Correlations between thin-section CT findings, histopathological and clinical findings of small pulmonary adenocarcinomas. *Lung Cancer* 2011; 71: 137–143. doi:10.1016/j.lungcan.2010.04.018.
- [16] Tateishi U, Kusumoto M, Nishihara H, Nagashima K, Morikawa T, Moriyama N. Contrast-enhanced dynamic computed tomography for the evaluation of tumor angiogenesis in patients with lung carcinoma. *Cancer* 2002; 95: 835–842. doi:10.1002/cncr.10730.
- [17] Ma SH, Le HB, Jia BH, et al. Peripheral pulmonary nodules: relationship between multi-slice spiral CT perfusion imaging and tumor angiogenesis and VEGF expression. *BMC Cancer* 2008; 8: 186. doi:10.1186/1471-2407-8-186.
- [18] Yi CA, Lee KS, Kim EA, et al. Solitary pulmonary nodules: dynamic enhanced multi-detector row CT study and comparison with vascular endothelial growth factor and microvessel density. *Radiology* 2004; 233: 191–199. doi:10.1148/radiol.2331031535.
- [19] Fraioli F, Anzidei M, Zaccagna F, et al. Whole-tumor perfusion CT in patients with advanced lung adenocarcinoma treated with conventional and antiangiogenic chemotherapy: initial experience. *Radiology* 2011; 259: 574–582. doi:10.1148/radiol.11100600.
- [20] Ohno Y, Koyama H, Matsumoto K, et al. Differentiation of malignant and benign pulmonary nodules with quantitative first-pass 320-detector row perfusion CT versus FDG PET/CT. *Radiology* 2011; 258: 599–609. doi:10.1148/radiol.10100245.
- [21] Xiong Z, Liu JK, Hu CP, Zhou H, Zhou ML, Chen W. Role of immature microvessels in assessing the relationship between CT perfusion characteristics and differentiation grade in lung cancer. *Arch Med Res* 2010; 41: 611–617. doi:10.1016/j.arcmed.2010.11.005.
- [22] Chae EJ, Song JW, Krauss B, et al. Dual-energy computed tomography characterization of solitary pulmonary nodules. *J Thorac Imaging* 2010; 5: 301–310.
- [23] Tacelli N, Remy-Jardin M, Copin MC, et al. Assessment of non-small cell lung cancer perfusion: pathologic-CT correlation in 15 patients. *Radiology* 2010; 257: 863–871. doi:10.1148/radiol.10100181.